METHODS

Our image base was created from orthorectified Landsat ETM+ images, sharpened to 15 m/pixel resolution. We selected images taken in April or May where possible, because vegetation cover differences are most marked at the end of the rainy season in Madagascar, providing maximum colour contrast between active gullies and non-lavaka'd terrain. We used 7-4-2 band composites, imported into ENVI for image processing. The band composites were first linearly enhanced, and then run through Gram-Spectral sharpening using the panchromatic band 8 (to which a median pass filter had first been applied). The sharpened images were projected in ArcMap 9.2, and further enhanced: first by applying a second pan-sharpening (simple mean) using the panchromatic band 8 image, and finally by increasing image brightness by 8-12% and increasing contrast by 45-55% (both adjustments via the "properties" function of the projected image layer).

We counted 60,946 lavakas on the Landsat images by systematic east-west lawnmowing on 33-km^2 panels (5 km x 6.5 km) at a scale of 1:25,000. Exposed laterite or saprolite—indicating active erosion—showed as dramatic pink in the enhanced images. Only active lavakas (those clearly showing exposed earth in their interiors) were included in our counts. Lavakas were distinguished from other gully or ravine types by their characteristic tadpole or inverted-teardrop shapes; and from non-gullied areas of bare ground by the combination of shape and shadowing indicating steep amphitheatre walls. We were able to ground truth our methodology for a variety of terrain types using the very high-resolution imagery available for some areas of Madagascar in Google Earth.

We estimate—by comparing our data with ≈2 m/pixel imagery available for limited areas of Madagascar in Google Earth—that our database is complete for the largest 50% of lavakas, and close to complete for the largest two-thirds. The median lavaka size is ≈1800 m^2 (based on field measurements of 433 lavakas: Wells et al., 1991; Wells, unpublished data; and Cox and Rakotondrazafy, unpublished data), which corresponds to 8 pixels. Lavakas <900 m^2 (4 pixels), representing about a third of lavakas (based on field measurements of 433 lavakas: Wells et al., 1991, and unpublished data), are underrepresented in our database because of resolution issues. Thus, we have a robust dataset for the largest two-thirds of lavakas.

We define the lavaka-prone area as the area within which all counted lavakas are contained (Fig DR 2). It represents that portion of Madagascar having the combination of climate, topography, and bedrock/weathering mantle geology required to support lavaka formation. The lavaka-prone area is ≈ 225000 km^2, or ≈40% of the total area of Madagascar. The main lavaka-prone area corresponds to the central highlands; and there is a small secondary lavaka-prone area (the Bekodoka dome: Figs. DR2, DR3) representing a hilly Precambrian basement outlier to the west. A polygon outlining the lavaka-prone area was used for subsequent operations on the raster datasets.

The seismic data were collected and processed by the Institut et Observatoire de Géophysique d'Antananarivo (Bertil and Regnoult, 1998; Ramanantsoa, 2000), and imported into ArcMap as X-Y co-ordinates. We plotted two different sets: 2174 events with magnitude 3.0-5.6, recorded 1979-1994 (Bertil and Regnoult, 1998); and 1268 events with magnitude 0.5-5.4, recorded in 1996 (Institut et Observatoire de Géophysique d'Antananarivo, 2008). All hypocentres are within the crust, and most are in the depth range 15-30 km (Rambolomanana et al., 1997; Bertil and Regnoult, 1998). The location error on each event ranges from 2-15 km (Bertil and Regnoult, 1998), but both the sample size (aggregate N = 3442) and the spatial scale of the earthquake clustering (Fig. 3) are large enough that this does not affect interpretation of the regional seismicity (e.g. Rambolomanana et al., 1997). The distribution densities of the two datasets are identical within error, and the aggregate N of 3442 provides a robust sample population from which to compute regional variations in overall seismicity. Of the 3442 events, 2738 occur within the lavaka-prone area; this subset is used to compute the relationship between lavaka and seismic density within the lavaka-prone area (Table DR1, Fig. 4). Magnitude and hypocentre depth are independent of location, and neither shows any correlation with lavaka distribution; so for this analysis we consdider only the bulk distribution of seismicity.

The spatial distributions of lavakas and seismic events were analysed using the Spatial Analyst kernel density function within ArcMap (Figs. DR2, DR3), and the Getis-Ord G_i* statistic (Ord and Getis, 1995; Getis and Ord, 1996). Getis-Ord analysis addresses spatial relationships among data, and tests for the existence and significance of data clusters or "hot spots" (Getis and Ord, 1996). Implementation of the Getis-Ord statistic requires weighted data, so we first converted the mapped lavaka and seismic event locations to local densities (using the kernel density function). The density raster data were converted to point data, with each point on the map representing the local feature density. These weighted point data were then input to the Getis-Ord analysis.

The Getis-Ord G_i* statistic is a Z score, representing the difference between the local sample and the weighted global mean of the data, divided by the weighted local standard deviation. Thus, G_i* is positive when a cluster has values higher than the mean, and negative when the values are lower. Although it is based on properties of the normal distribution, the test does not require that the underlying data are normally distributed: as long as the sample size is sufficiently large, the results of the statistical test are asynptotically normal (Lin, 2004). The critical value for 95% confidence that clustering exists is $G_i^* > +1.96$. The clustering of lavakas (Fig. 2) and of seismic events (Fig. 3) is clearly demonstrated by the magnitude of the G_i* values: areas shown in red have G_i^* >10, i.e. more than 10 standard deviations from the mean, representing exceptionally dense clustering.

To quantify the distriburion of lavakas as a funcion of seismic acrivity, we reclassified the seismic kernel density raster data and converted them to polygons, each representing an area characterised by a specific seismic density range. We cropped those portions of the seismic density polygons that fell outside the lavaka-prone area, and also excluded the area occupied by Lac Alaotra, thereby constraining the seismicity-lavaka analysis to those areas where bedrock geology, topography, and climate combine to make lavaka activity possible[*].

We measured the polygon sizes to get the total area represented by each seismic density bracket. As the brackets were derived from a probability density function superimposed on the data (thus nominal rather than actual representations of the true

[*] We note that the same lavaka vs. seismic density patterns result whether or not the analysis is restricted to the lavaka-prone area: because all lavakas and most seismicity are restricted to the central spine of Madagascar, a straight nationwide correlation produces the same logarithmic trend. But the analysis is tighter and more representative of the underlying connections when restricted to the central uplands.

seismic densities), we went back and counted the absolute number of seismic events captured in each bracket. Thence we calculated the actual seismic densities for those areas. Finally, we counted the number of lavakas occurring in each polygon, from which we calculated the lavaka density for each seismic density bracket (Table DR 1).

REFERENCES

Bertil, D., and Regnoult, J.M., 1998, Seismotectonics of Madagascar: Tectonophysics, v. 294, p. 57-74.

Getis, A., and Ord, J.K., 1996, Local spatial statistics: an overview, *in* Longley, P., and Batty, M., eds., Spatial Analysis: Modeling in a GIS Environment: Cambridge, Geoinformation International, p. 261-277.

Institut et Observatoire de Géophysique d'Antananarivo, 2008, Liste des seismes locaux enregistres par le reseau sismique Malgache en 1996: http://www.refer.mg/edu/minesup/antanana/ioga/sisdata.htm.

IOGA, 2008, Liste des seismes locaux enregistres par le reseau sismique Malgache en 1996: Institut et Observatoire de Géophysique d'Antananarivo: http://www.refer.mg/edu/minesup/antanana/ioga/sisdata.htm.

Le Bourdiec, F., Battistini, R., and LeBourdiec, P., 1971, Atlas de Madagascar: Tananarive, Bureau pour le Development de la Production Agricole, 120 p.

Lin, G., 2004, Comparing spatial clustering tests based on rare to common spatial events: Computers, Environment, and Urban Systems, v. 28, p. 691-699. doi:10.1016/j.compenvurbsys.2003.07.002.

Ord, J.K., and Getis, A., 1995, Local spatial autocorrelation statistics: Distributional issues and an application: Geographical Analysis, v. 27, p. 286-306.

Ramanantsoa, A.H., 2000, Seismic observation in Madagascar: Bulletin of the International Institute of Seismology and Earthquake Engineering, v. 34, p. 59-69.

Rambolomanana, G., Suhadolc, P., and Panza, G.F., 1997, Simultaneous inversion of hypocentral parameters and structure velocity of the central region of Madagascar as a premise for the mitigation of seismic hazard in Antananarivo: Pure and Applied Geophysics, v. 149, p. 707-730.

Wells, N.A., 2003, Some hypotheses on the Mesozoic and Cenozoic paleoenvironmental history of Madagascar, *in* Goodman, S.M., and Benstead, J.P., eds., The Natural History of Madagascar: Chicago, University of Chicago Press, p. 16-34.

Wells, N.A., Andriamihaja, B., and Rakotovololona, H.F.S., 1991, Patterns of development of lavaka, Madagascar's unusual gullies: Earth Surface Processes and Landforms, v. 16, p. 189-206.

SUPPLEMENTAL MATERIAL FIGURE CAPTIONS

Fig. DR1: Examples of areas with similar convex-hill topography but differing local lavaka densities. Image A is centred at appoximately 18.53°S 47.78°E, and B is centred at approximately 17.36°S, 47.86°E. (locations are shown on Fig. 2). The two areas have the same climate: both have >1500 mm of rainfall per year, mean cold-month low temperatures of 10-15°C, and 3-4 dry months per year (Le Bourdiec et al., 1971; Wells, 2003). Valley bottoms in image B are broad and flat, reflecting high local sedimentation rates due to lavaka actiity. These images serve also as an illustration of the lack of connection between human activity and lavaka formation. Image A, with no lavakas, has substantial human habitation and land use, a greater density of roads and tracks, a wide range of field types on the hills, and extensive evidence for unvegetated bare earth (pale pink patches and mottling on the hillslopes). Image B, in contrast, has very little habitation and agriculture (there are a few fields in some of the valleys, and a couple of huts in white circular areas on ridge crests), few tracks, and few areas of bare or distrurbed ground; yet lavakas are abundant. Image A is 50 km northeast of Antananrivo, slightly east of the lavaka hotspot region (Fig. 2). Image B , however, about 40 km east of Andriamena, is within one of the largest hotspot areas (Fig. 2), spatially associated with the Lac Alaotra seismic hotspot region (Fig. 3), which has the greatest earthquake densities in Madagascar. Image A, with no active lavakas, has in fact been extensively lavaka'd in the past: many ancient lavakas can be distinguished by their rounded amphitheatrical headwalls and narrow outlets (one example is labelled “AL”). Image B has very few of these features. Images © 2008 Europa Technologies, Digital Globe, and Google Earth; reproduced by fair-use permission (www.google.com/permissions/geoguidelines.html).

Fig. DR2: Density distribution for lavakas in Madagascar. We mapped Madagascar's large lavakas from Landsat images at 15 m/pixel resolution, generating a database of 60,946 individual lavaka locations from which we computed the density distribution (see Supporting Online Matieral: Methods). Because of image resolution, only the largest ≈2/3 of lavakas are represented by the numerical densities; but the relative densities and distribution patterns are representative of the general lavaka population. The lavaka-prone area is defined as the area inside the envelopes that enclose all the datapoints, and represents ≈40% of the total area of Madagascar. Spatial statistical analysis of the data is shown in main manuscript Fig. 2.

Fig. DR3: Density distribution for 3442 sesimic events (magnitudes 0.5-5.6), recorded between 1979-1994 (Bertil and Regnoult, 1998; Ramanantsoa, 2000), and in 1996 (IOGA, 2008). The densities are nominal, not absolute, because they represent the period of record only; but the dataset is sufficiently large to represent a robust proxy for long-term seismic activity (Bertil and Regnoult, 1998). Of the 3442 events, 2738 (80%) occur within the lavaka-prone area (outline shown). Spatial statistical analysis of the data is shown in main manuscript Fig. 3.

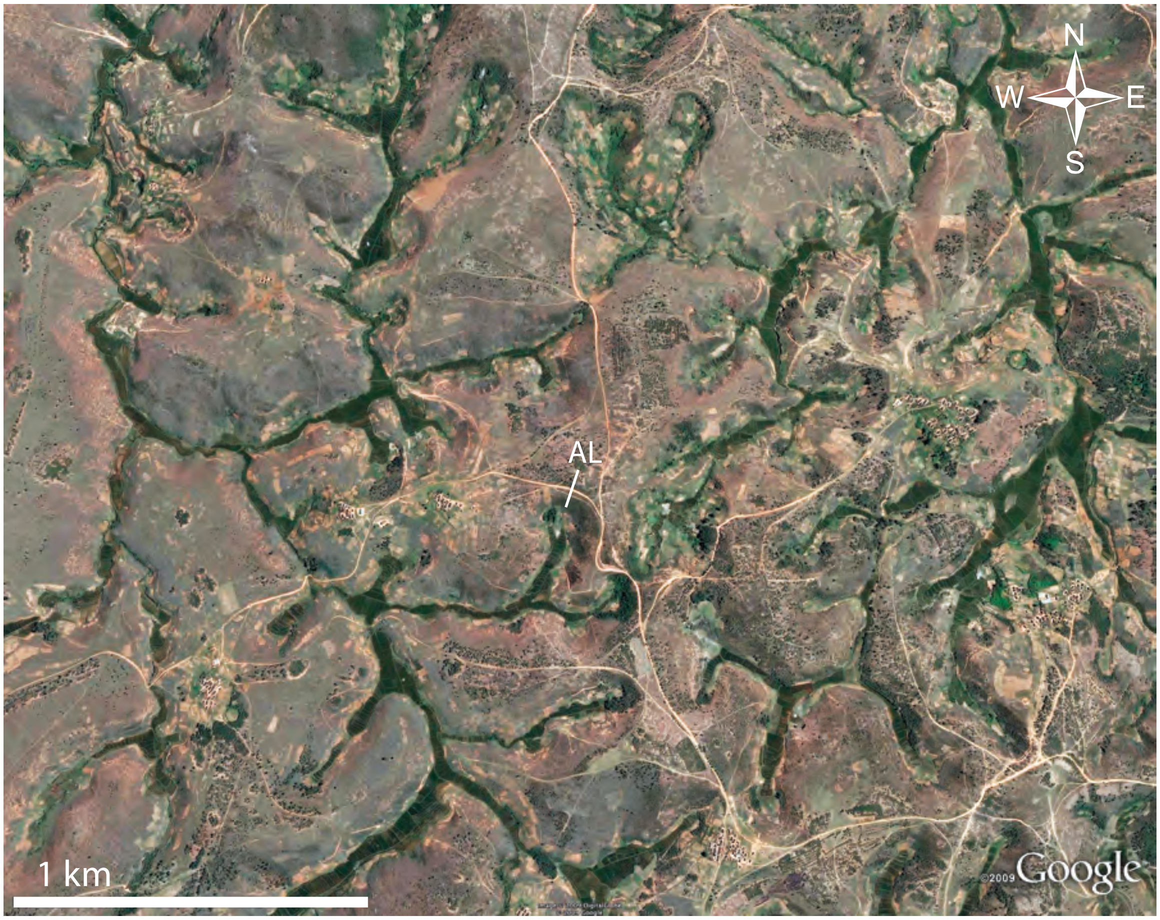
N
W
E
S
AL
1 km
©2009 Google

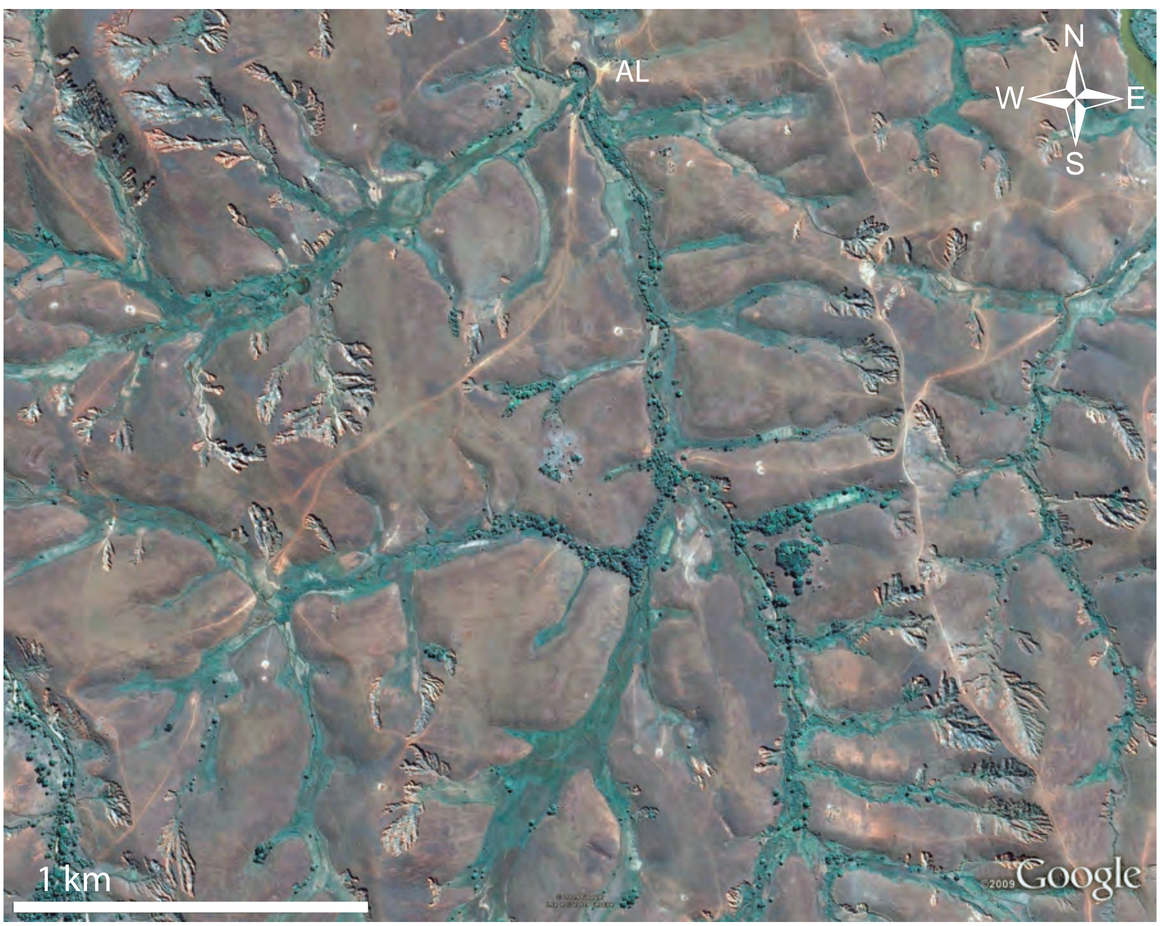
N
W
E
S
AL
1 km
©2009 Google

Cox et al. Fig. DR 2

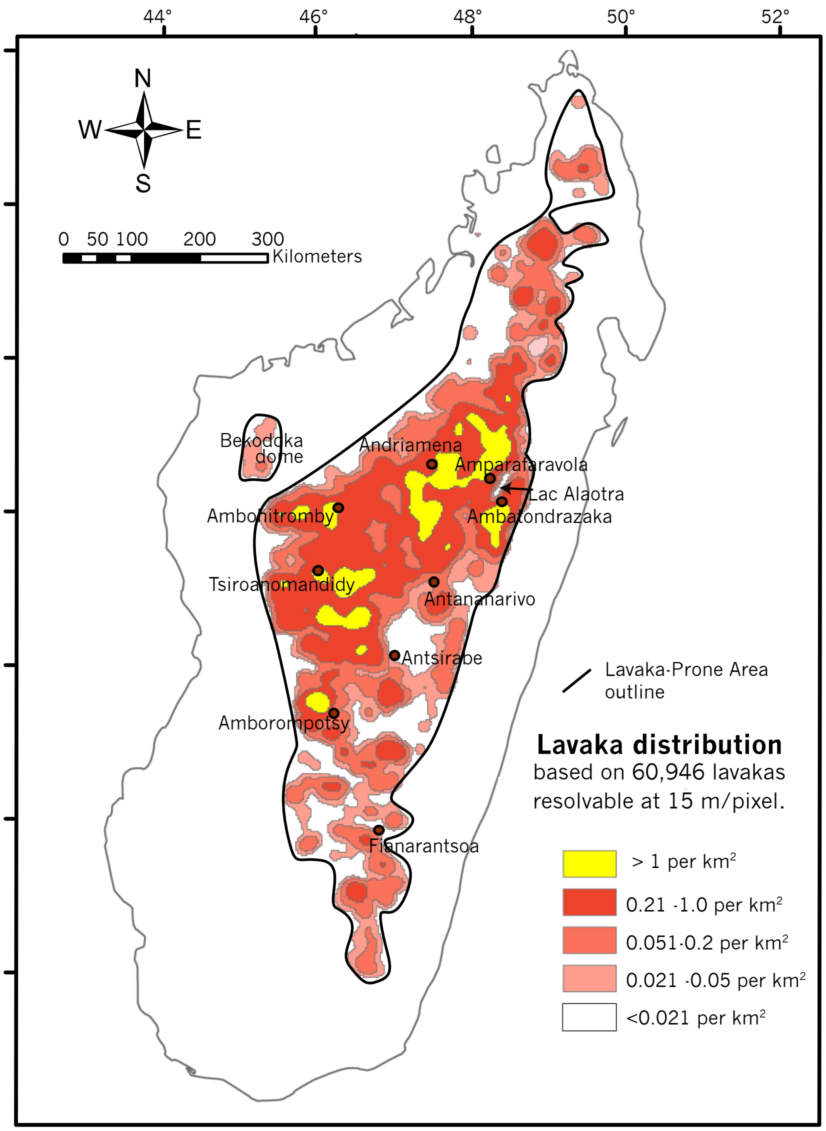

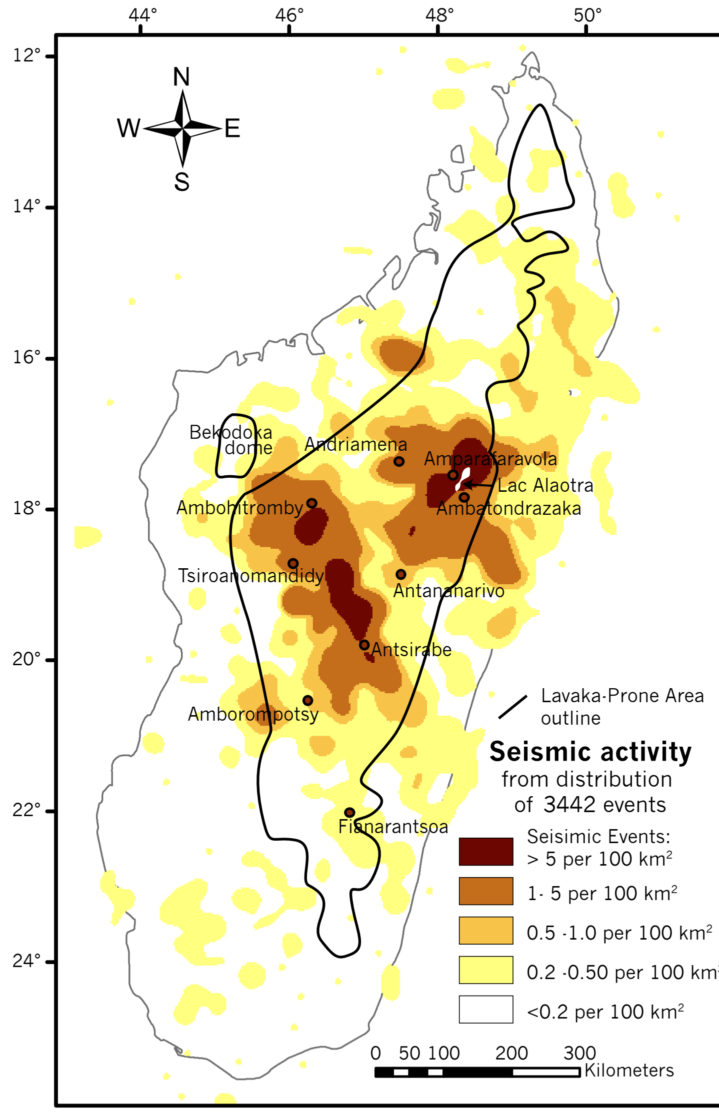
44°
46°
48°
50°
12°
14°
16°
18°
20°
22°
24°
N
W
E
S
Bekodoka dome
Andriamena
Amparafaravola
Lac Alaotra
Ambatondrazaka
Ambohitromby
Tsiroanomandidy
Antananarivo
Antsirabe
Amborompotsy
Fianarantsoa
Lavaka-Prone Area outline
Seismic activity
from distribution of 3442 events
Seisimic Events:
> 5 per 100 km²
1- 5 per 100 km²
0.5 -1.0 per 100 km²
0.2 -0.50 per 100 km²
<0.2 per 100 km²
0 50 100 200 300
Kilometers

Table DR 1. Densities of seismic events and lavakas within the lavaka-prone area (LPA). The total number of lavakas is 60,946, and the total number of seismic events is within the LPA is 2738. Densities are nominal: they represent lavakas resolvable at 15 m/pixel, and sesimic events from two discrete collection inervals. Data were analysed using ArcMap. See Methods section for more information.

†Seismic density bracket	*Area (km^2)	Number of seismic events	§Seismic events per $100km^2$	Number of lavakas	Lavakas/km^2
1	60,797	0	0	5242	0.09
2	27,472	33	0.1	2505	0.09
3	19,220	33	0.2	3525	0.18
4	11,472	58	0.4	2562	0.22
5	14,821	42	0.4	2726	0.18
6	4,952	54	0.6	1649	0.33
7	3,852	46	0.6	1349	0.35
8	8,637	44	0.6	2201	0.25
9	7,270	28	0.6	2073	0.29
10	5,849	23	0.8	1850	0.32
11	25,351	320	1.3	11734	0.46
12	13,573	314	2.3	10018	0.74
13	8,248	280	3.4	5506	0.67
14	4,814	227	4.7	2574	0.53
15	2,433	148	6.1	1345	0.55
16	1,825	147	8.1	1008	0.55
17	983	149	8.7	511	0.52
18	490	86	9.6	244	0.50
19	1,493	47	10	1114	0.75
20	1,186	508	43	1199	1.01
21	5	151	3020	11	2.20

†Equal-interval brackets from kernel density function in ArcMap
*LPA only. Total LPA ≈ 225,000 km^2, i.e. ≈40% of the area of Madagascar.
§ Absolute number of seismic events occuring in each density bracket, divided by area